

# The Neuroprotective Effect of 2-(3-Pyridyl)-1-azabicyclo[3.2.2]nonane (TC-1698), a Novel $\alpha 7$ Ligand, Is Prevented through Angiotensin II Activation of a Tyrosine Phosphatase

Mario B. Marrero, Roger L. Papke, Balwinder S. Bhatti, Seán Shaw, and Merouane Bencherif

*Department of Pharmacology and Toxicology (M.B.M.), Vascular Biology Center, Medical College of Georgia, Augusta, Georgia (M.B.M., S.S.); Department of Physiology and Pharmacology, University of Florida, Gainesville, Florida (R.L.P.); and Department Preclinical Research (M.B.) and Drug Discovery and Development (B.S.B.), Targacept Inc., Winston-Salem, North Carolina*

Received October 16, 2003; accepted December 10, 2003

## ABSTRACT

We have recently provided evidence for nicotine-induced complex formation between the  $\alpha 7$  nicotinic acetylcholine receptor (nAChR) and the tyrosine-phosphorylated enzyme Janus kinase 2 (JAK2) that results in subsequent activation of phosphatidylinositol-3-kinase (PI-3-K) and Akt. Nicotine interaction with the  $\alpha 7$  nAChR inhibits  $A\beta$  (1-42) interaction with the same receptor, and the  $A\beta$  (1-42)-induced apoptosis is prevented through nicotine-induced activation of JAK2. These effects can be shown by measuring markers of cytotoxicity, including the cleavage of the nuclear protein poly(ADP-ribose) polymerase (PARP), the induction of caspase 3, or cell viability. In this study, we found that 2-(3-pyridyl)-1-azabicyclo[3.2.2]nonane (TC-1698), a novel  $\alpha 7$ -selective agonist, exerts neuroprotective effects via activation of the JAK2/PI-3K cascade, which can be neutralized through activation of the angiotensin II (Ang II)  $AT_2$  receptor.

Vanadate not only augmented the TC-1698-induced tyrosine phosphorylation of JAK2 but also blocked the Ang II neutralization of TC-1698-induced neuroprotection against  $A\beta$  (1-42)-induced cleavage of PARP. Furthermore, when SHP-1 was neutralized via antisense transfection, the Ang II inhibition of TC-1698-induced neuroprotection against  $A\beta$  (1-42) was prevented. These results support the main hypothesis that states that JAK2 plays a central role in the nicotinic  $\alpha 7$  receptor-induced activation of the JAK2-PI-3K cascade in PC12 cells, which ultimately contribute to nAChR-mediated neuroprotection. Ang II inhibits this pathway through the  $AT_2$  receptor activation of the protein tyrosine phosphatase SHP-1. This study supports central and opposite roles for JAK2 and SHP-1 in the control of apoptosis and  $\alpha 7$ -mediated neuroprotection in PC12 cells.

Neuronal nicotinic acetylcholine receptors (nAChRs) are composed of various combinations of  $\alpha$ -subunits ( $\alpha 2$ - $\alpha 10$ ) and  $\beta$ -subunits ( $\beta 2$ - $\beta 4$ ) that form homo- or heteropentamers. The  $\alpha 7$  nAChR forms functional homomeric ligand-gated ion channels that promote rapidly desensitizing  $Ca^{2+}$  influx, is widely expressed throughout the mammalian brain, and has been implicated in sensory gating, cognition, inflammation,

and neuroprotection (Kem, 2000; Bencherif and Schmitt, 2002; Kitagawa et al., 2003; Wang et al., 2003). The cholinergic deficit in neurodegenerative diseases has been clearly established and is the basis for current therapeutic strategies. There is an early and significant depletion of high-affinity nicotinic receptors in the brains of Alzheimer's patient's (Breese et al., 1997; Court et al., 2001), with a selective loss of nAChR predominating in brain regions with  $\beta$ -amyloid deposition. Several studies have shown cognitive improvement in rodents and primates, including humans, after administration of ligands targeting nicotinic acetylcholine receptors (Newhouse et al., 2001). In addition to their known symptomatic effects, neuronal nicotinic ligands have shown

This work was supported by Targacept Inc. (to M.B.M., R.L.P., S.S.), and in part by National Institutes of Health Grants HL58139 and DK50268 (to M.B.M.), the American Heart Association Established Investigator Award (to M.B.M.), and National Institutes of Health Grant PO1 AG10485 (to R.L.P.).

Article, publication date, and citation information can be found at <http://jpet.aspetjournals.org>.

DOI: 10.1124/jpet.103.061655.

**ABBREVIATIONS:** nAChR, nicotinic acetylcholine receptor; PI-3-K, phosphatidylinositol-3-kinase; MAPK, mitogen-activated protein kinase; JAK2, Janus kinase 2; PARP, poly(ADP-ribose) polymerase; Ang II, angiotensin II; PTPase, protein tyrosine phosphatase; PMSF, phenylmethylsulfonyl fluoride; PBS, phosphate-buffered saline; BSA, bovine serum albumin; MLA, methyllycaconitine; ACh, acetylcholine; PAGE, polyacrylamide gel electrophoresis; TTBS, Tris-Tween 20-buffered saline; IL, interleukin; PD 123,177, S(+)-1-[(4-amino-3-methylphenyl)methyl]-5-(diphenylacetyl)-4,5,6,7-tetrahydro-1H-imidazo-(4,5-c)pyridine-6-carboxylic acid; AG-490,  $\alpha$ -cyano-(3,4-dihydroxy)-N-benzylcinnamide.

neuroprotective activity *in vitro* and *in vivo*, suggesting an additional potential for disease modification (Donnelly-Roberts et al., 1996; Kihara et al., 2001; Nordberg et al., 2002). A direct interaction of the  $\beta$ -amyloid peptide with the  $\alpha 7$  nAChR is suggested by recent findings.  $\beta$ -Amyloid peptide interacts with high affinity to the  $\alpha 7$  nAChR and results in functional noncompetitive blockade in hippocampal neurons (Wang et al., 2000; Liu et al., 2001). In addition, nicotine-induced neuroprotection against  $\beta$ -amyloid induced toxicity is suppressed by  $\alpha$ -bungarotoxin, and selective  $\alpha 7$  nAChR agonists exert cytoprotective effects (Kem, 2000; Shaw et al., 2002).

Recent studies have reported that  $\alpha 7$ -mediated effects are mediated through phosphorylation of specific kinases such as Akt and subsequent activation of phosphatidylinositol 3-kinase (Kihara et al., 2001). Another study has shown that whereas nicotine activates the PI-3-K neuroprotective cascade,  $A\beta$  (1-42) chronically activates the mitogen-activated protein kinase (MAPK) cascade via the hippocampal  $\alpha 7$  nAChR (Dineley et al., 2001). These findings were interpreted as evidence that chronic activation of the MAPK pathway by  $A\beta$  (1-42) eventually leads to the down-regulation of MAPK, which then sets up a positive feedback for  $A\beta$  accumulation and decreased phosphorylation of the cAMP regulatory protein (cAMP response element-binding protein), which is a necessary component for hippocampus-dependent memory formation in mammals. Nonetheless, these findings suggest that the  $\alpha 7$  nAChR transduces signals to PI-3-K in a cascade, which ultimately contributes to a neuroprotective effect against  $A\beta$  (1-42).

There is recent evidence for the nicotine-induced complex formation between the  $\alpha 7$  nAChR and the tyrosine-phosphorylated enzyme JAK2 that results in subsequent activation of PI-3-K and Akt (Shaw et al., 2002). In addition, nicotine interaction with the  $\alpha 7$  nAChR is "dominant" over  $A\beta$  (1-42) interaction with the receptor, and the  $A\beta$  (1-42)-induced apoptosis is

prevented through the nicotine-induced activation of JAK2. These effects can be shown by measuring markers of cytotoxicity such as the cleavage of the nuclear protein PARP, the induction of caspase 3, or cell viability. Finally, we reported that neuroprotective effects of nicotine could be neutralized through activation of the angiotensin II AT<sub>2</sub> receptor as evidenced by the reversal of JAK2 phosphorylation and inhibition of nicotine-induced neuroprotection (Shaw et al., 2002).

In this study, we report that 2-(3-pyridyl)-1-azabicyclo [3.2.2]nonane (TC-1698) is a highly selective nicotinic  $\alpha 7$  receptor agonist that it activates JAK2 in PC12 cells and that this activation and downstream activation of PI-3-K and Akt are blocked by the specific inhibitor AG490. TC-1698-induced phosphorylation of JAK2 can be neutralized through angiotensin II (Ang II)-activation of the AT<sub>2</sub> receptor and these effects are mediated through the protein tyrosine phosphatase (PTPase) SHP-1. Furthermore, usage of the PTPase SHP-1 antisense identified central and opposite roles for Jak2 and SHP-1 in the control of  $\alpha 7$  nAChR-mediated PC12 cell survival and apoptosis.

## Materials and Methods

### Synthetic Procedures

The compound TC-1698 was prepared by the alkylation of the imine derived from 3-acetylpyridine and isopropylamine. Thus, the sequential treatment of imine with lithium diisopropyl amide and 4-(bromomethyl)oxane provided the key intermediate 1-(3-pyridyl)-2-(4-oxanyl)propan-1-one, which was readily elaborated into the higher homolog of 2-(3-pyridyl)-quinuclidines. The construction of the [3.2.2] ring was accomplished by the transformation of the intermediate into oxime (1-pyridin-3-yl-3-(tetrahydropyran-4-yl)-propan-1-one oxime) and then to the amine 1-pyridin-3-yl-3-(tetrahydropyran-4-yl)-propylamine. The amine upon heating with concentrated HBr in a sealed tube, followed by removal of the acid, and then refluxing with dilute ethanolic potassium carbonate yielded TC-1698 (Fig. 1). The structure was confirmed by <sup>1</sup>H and <sup>13</sup>C NMR, gas chro-

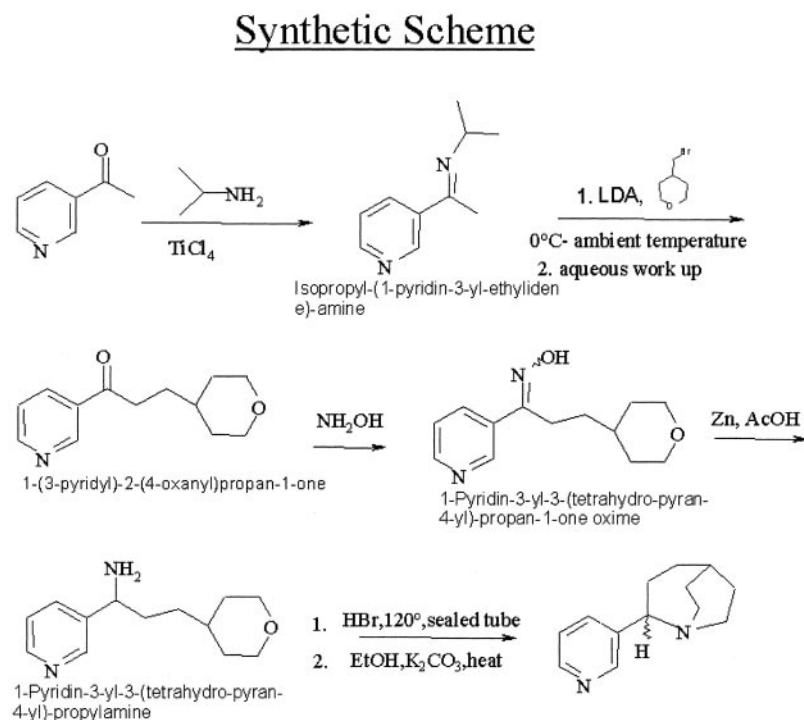


Fig. 1. Synthetic scheme for TC-1698.

matography-mass spectrometry, and elemental analysis as 2-(3-pyridyl)-1-azabicyclo[3.2.2]nonane dihydrochloride (TC-1698) as 99.9% pure.

## Binding Studies

**Tissue Preparation.** Rats were killed by decapitation after anesthesia with 70% CO<sub>2</sub>. The brain was rapidly removed and placed on an ice-cold platform. The cerebral cortex, cerebellum, hippocampus, and striatum regions were dissected and stored at -20°C until use for membrane preparation.

**Preparation of Membranes from Rat Tissues.** Tissue was homogenized in 10 vol (w/v) of ice-cold preparative buffer (11 mM KCl, 6 mM KH<sub>2</sub>PO<sub>4</sub>, 137 mM NaCl, 8 mM Na<sub>2</sub>HPO<sub>4</sub>, 20 mM HEPES, 5 mM iodoacetamide, 1.5 mM EDTA, and 0.1 mM PMSF, pH 7.4, using a Polytron (Brinkmann Instruments, Westbury, NY) at setting 6 for 15 s. The homogenate was then be centrifuged at 40,000g for 20 min at 4°C, the pellet was resuspended in 20 vol of ice-cold water, and incubated for 20 min at 4°C. The final pellet (40,000g for 20 min at 4°C) was then be resuspended in preparative buffer and stored at -20°C. On the day of assay, tissue was thawed, centrifuged at 40,000g for 20 min at 4°C, and then resuspended in Dulbecco's phosphate-buffered saline (PBS, #21300; Invitrogen, Carlsbad, CA), pH 7.4, to a final concentration of 2 to 3 mg/ml total protein. PBS with 0.05% BSA was used to resuspend hippocampal membranes. Protein concentration was determined by the Bradford method using BSA as the standard.

**[<sup>3</sup>H]Methyllycaconitine (MLA) and [<sup>3</sup>H]Nicotine Binding Assays.** The [<sup>3</sup>H]MLA binding assay was used to detect and quantify the α7 nAChRs in cerebral cortex, cerebellum, hippocampus, and striatum as described previously (Davies et al., 1999). Briefly, each sample (150 μl of total volume) consisted of membrane suspension (~150 μg of protein), 5 nM [<sup>3</sup>H]MLA for single-point screening, or 0.5 to 20 nM for the saturation analysis. Nonspecific binding was determined in the presence of 10 μM cold MLA. Binding reactions were conducted for 2 h at room temperature in 96-well microtiter plates in triplicate. The binding reaction was terminated by rapid filtration onto Whatman GF/B glass fiber filters, presoaked in 0.3% polyethyleneimine, using a tissue harvester (Brandel Inc., Gaithersburg, MD). After washing five times with ~350 μl of the ice-cold PBS, the filter plate was dried at 49°C for approx. 2 h. MeltiLex A melt-on scintillator sheets (PerkinElmer Life Sciences, Boston, MA) were then be applied to the dry filters, and radioactivity bound to the membranes was determined by liquid scintillation counting. The [<sup>3</sup>H]nicotine binding assay used the same procedure to detect and quantify α4β2 nAChRs (Romano and Goldstein, 1980).

## Preparation of RNA

The human nAChR clones were obtained from Dr. Jon Lindstrom (University of Pennsylvania, Philadelphia, PA) and the mouse muscle subunit clones were from Dr. Jim Boulter (University of California, Los Angeles, Los Angeles, CA); the mouse epsilon clone was provided by Dr. Paul Gardener (University of Massachusetts Medical School, Worcester, MA). After linearization and purification of cloned cDNAs, RNA transcripts were prepared in vitro using the appropriate mMessage mMachine kit from Ambion (Austin, TX).

## Expression in *Xenopus* Oocytes

Mature (>9 cm) female *X. laevis* African toads (Nasco, Ft. Atkinson, WI) were used as a source of oocytes. Before surgery, frogs were anesthetized by placing the animal in a 1.5 g/l solution of 3-aminobenzoic acid ethyl ester for 30 min. Oocytes were removed from an incision made in the abdomen. To remove the follicular cell layer, harvested oocytes were treated with 1.25 mg/ml collagenase from Worthington Biochemicals (Freehold, NJ) for 2 h at room temperature in calcium-free Barth's solution (88 mM NaCl, 10 mM HEPES, pH 7.6, 0.33 mM MgSO<sub>4</sub>, and 0.1 mg/ml gentamicin sulfate). Subsequently, stage 5 oocytes were isolated and injected with 50 nl (5–20

ng) each of the appropriate subunit cRNAs. Recordings were made 1 to 15 days after injection.

## Electrophysiology

Experiments were conducted using a beta version of OpusXpress 6000A (Axon Instruments, Union City, CA). OpusXpress is an integrated system that provides automated impalement and voltage clamp of up to eight oocytes in parallel. The beta unit used for these studies recorded from four cells simultaneously. Cells were automatically perfused with bath solution, and agonist solutions were delivered from a 96-well plate. Both the voltage and current electrodes were filled with 3 M KCl. The agonist solutions were applied via disposable tips, which eliminated any possibility of cross-contamination. Drug applications alternated between ACh controls and experimental applications. Flow rates were set at 1 ml/min. Cells were voltage-clamped at a holding potential of -60 mV. Data were collected at 50 Hz and filtered at 20 Hz. Drug applications were 20 s in duration followed by 383-s washout periods for α7 receptors and 10 s with 383-s wash periods for other subtypes.

## Experimental Protocols and Data Analysis

Each oocyte received two initial control applications of ACh and an experimental drug application, and then a follow-up control application of 300 μM ACh. The control ACh concentrations for α1β1εδ, α3β4, α4β2, α3β2, and α7 receptors were 30, 100, 10, 30, and 300 μM, respectively. These concentrations were determined to be the EC<sub>74</sub>, EC<sub>15</sub>, EC<sub>22</sub>, EC<sub>18</sub>, and EC<sub>100</sub>, respectively. Responses to TC-1698 applications were calculated relative to the preceding ACh control responses to normalize the data, compensating for the varying levels of channel expression among the oocytes. Drug responses were initially normalized to the ACh control response values and then adjusted to reflect the TC-1698 responses relative to the ACh maximums. Responses for α7 receptors were calculated as net charge over a 90-s interval, beginning with the drug application (Papke and Papke, 2002). For subtypes other than α7, responses were calculated from the peak current amplitudes. Means and S.E.M. were calculated from the normalized responses of at least three oocytes for each experimental concentration. The application of some experimental drugs caused the subsequent ACh control responses to be reduced, suggesting some form of residual inhibition (or prolonged desensitization). To measure the residual inhibitory effects, this subsequent control response was compared with the preapplication control ACh response.

For concentration-response relations, data derived from net charge analyses were plotted using KaleidaGraph 3.0.2 (Abelbeck Software, Reading, PA), and curves were generated from the Hill equation as follows:

$$\text{Response} = \frac{I_{\max}[\text{agonist}]^n}{[\text{agonist}]^n + (\text{EC}_{50})^n}$$

where  $I_{\max}$  denotes the maximal response for a particular agonist/subunit combination, and  $n$  represents the Hill coefficient.  $I_{\max}$ ,  $n$ , and the  $\text{EC}_{50}$  were all unconstrained for the fitting procedures. Negative Hill slopes were applied for the calculation of  $\text{IC}_{50}$  values.

## Materials and Chemicals

Chemicals for electrophysiology were obtained from Sigma-Aldrich (St. Louis, MO) with the exception of TC-1698, which was synthesized. Other chemicals were purchased from Aldrich Chemical Co. (Milwaukee, WI). These were used without further purification, except in the case of tetrahydrofuran, which was dried by distillation from sodium and benzophenone. Merck silica gel 60 (70–230 mesh) was used for all the chromatographic purifications. Molecular weight standards, SDS, *N,N'*-methylene-bisacrylamide, *N,N,N',N'*-tetraethylenediamine, protein assay reagents, and nitrocellulose membranes were purchased from Bio-Rad (Hercules, CA). Protein A/G-agarose was obtained from Santa Cruz Biotechnology, Inc. (Santa

Cruz, CA), whereas Dulbecco's modified Eagle's medium (DMEM; Invitrogen), fetal bovine serum (Atlanta Biologicals, Norcross, GA), and trypsin and all medium additives were obtained from Mediatech (Herndon, VA). Monoclonal antibody to phosphotyrosine (PY20) and SHP-2 were procured from BD Biosciences Transduction Laboratories (Lexington, KY). PARP antibodies were purchased from New England Biolabs (Beverly, MA). Anti-phosphotyrosine JAK2 and JAK2 antibodies were obtained from BioSource International (Camarillo, CA). The Supersignal substrate chemiluminescence detection kit was obtained from Pierce Chemical (Rockford, IL). Goat anti-mouse IgG and anti-rabbit IgG were acquired from Amersham Biosciences Inc. (Princeton, NJ), and Tween 20, A $\beta$  (1-42) peptide, anti-A $\beta$  (1-42), and anti- $\alpha$ 7 nAChR and all other chemicals were purchased from Sigma-Aldrich.

### Isolation and Culture of PC12 Cells

PC12, rat pheochromocytoma cells, were maintained in proliferative growth phase in Dulbecco's modified Eagle's medium supplemented with 10% horse serum, 5% fetal calf serum, and antibiotics (penicillin/streptomycin) according to routine protocols (Bencherif et al., 1996).

### Western Blotting Studies of JAK2

The tyrosine phosphorylation of JAK2 was determined in serum-starved PC12 cells stimulated with 10  $\mu$ M TC-1698 (0–60 min) in the presence or absence of 10  $\mu$ M (1-h preincubation) of the JAK2 specific inhibitor AG-490 (Meydan et al., 1996; Dicou et al., 2001). Although many tyrosine kinase inhibitors are often promiscuous in the enzyme they target, AG-490 is unique in that it does not inhibit other tyrosine kinases such as Lck, Lyn, Btk, Syk, Src, JAK1, or Tyk2 (Meydan et al., 1996). At the end of stimulation, cells were washed twice with ice-cold phosphate-buffered saline with 1 mM Na<sub>3</sub>VO<sub>4</sub>. Each dish was then treated for 60 min with ice-cold lysis buffer (20 mM Tris-HCl, pH 7.4, 2.5 mM EDTA, 1% Triton X-100, 10% glycerol, 10 mM Na<sub>4</sub>P<sub>2</sub>O<sub>7</sub>, 50 mM NaF, 1 mM Na<sub>3</sub>VO<sub>4</sub>, and 1 mM PMSF), and the supernatant fraction was obtained as cell lysate by centrifugation at 58,000g for 25 min at 4°C. Samples were resolved by 10% SDS-PAGE, transferred to a nitrocellulose membrane, and blocked by 60-min incubation at 22°C in TTBS (Tris-buffered saline with 0.05% Tween 20, pH 7.4) plus 5% skimmed milk powder. The nitrocellulose membrane was incubated overnight at 4°C with affinity-purified anti-phospho specific JAK2 antibodies. The nitrocellulose membranes were washed 10 min twice with TTBS and incubated with goat anti-rabbit IgG horseradish peroxidase conjugate. After extensive washing, the bound antibody was visualized on a Kodak Biomax film using a Supersignal substrate chemiluminescence detection kit (Pierce Chemical).

### Immunoprecipitation Studies of SHP-1

The cell lysate prepared as described above was incubated with 10  $\mu$ g/ml anti-SHP-1 monoclonal antibodies at 4°C for 2 h and precipitated by addition of 50  $\mu$ l of protein A/G-agarose at 4°C overnight. The immunoprecipitates was recovered by centrifugation and washed three times with ice-cold wash buffer (Tris-buffered saline, 0.1% Triton X-100, 1 mM PMSF, and 1 mM Na<sub>3</sub>VO<sub>4</sub>). Immunoprecipitated proteins were dissolved in 100  $\mu$ l of Laemmli sample buffer, and 80  $\mu$ l of each sample was resolved by SDS-PAGE. Samples were transferred to a nitrocellulose membrane and blocked by 60-min incubation at room temperature (22°C) in TTBS plus 5% skimmed milk powder. The nitrocellulose membrane was then incubated overnight at 4°C with 10  $\mu$ g/ml affinity-purified anti-phosphotyrosine antibodies. The nitrocellulose membranes were washed for 10 min twice with TTBS and incubated with goat anti-mouse IgG horseradish peroxidase conjugate. After extensive washing, the bound antibody was visualized on a Kodak Biomax film using a Supersignal substrate chemiluminescence detection kit (Pierce Chemical).

### SHP-1 Tyrosine Phosphatase Activity Assay

SHP-1 activity was determined as described previously (Marrero et al., 1998). Briefly, SHP-1 proteins were immunoprecipitated with anti-SHP-1 antibodies from PC12 cell lysates, and the immunocomplexes were washed three times with ice-cold wash buffer and then three times with phosphatase buffer (50 mM HEPES, 60 mM NaCl, 60 mM KCl, 0.1 mM PMSF, 10  $\mu$ g/ml aprotinin, and 10  $\mu$ g/ml leupeptin, pH 7.4). Phosphatase activity was measured by monitoring the rate of formation of *p*-nitrophenol by dephosphorylation of *p*-nitrophenyl phosphate. Immunocomplex pellets were thus resuspended in 100  $\mu$ l of phosphatase buffer containing 1 mg/ml BSA, 5 mM EDTA, and 10 mM dithiothreitol. The reaction was initiated by the addition of *p*-nitrophenyl phosphate (10 mM final concentration). After a 30-min incubation at room temperature, the reaction was stopped by the addition of 1 M NaOH, and absorbance of the sample was determined at 410 nm in a spectrophotometer.

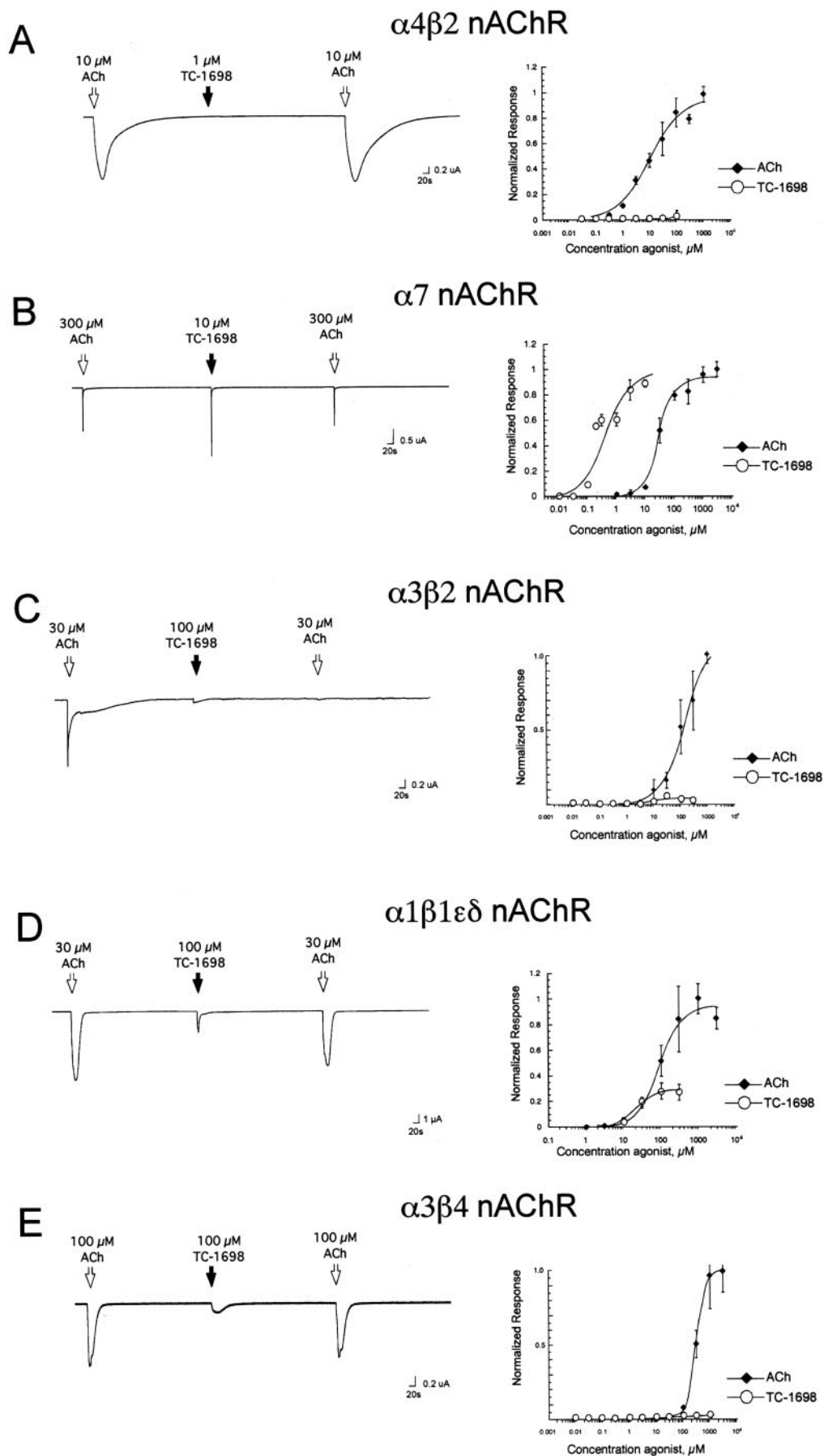
### Antisense against SHP-1

An antisense oligonucleotide that targets the translational start site of the murine SHP-1 coding sequence (5'-ACCTCACCATCCTTGGGGT-3') has been found to significantly reduce SHP-1 expression in human erythroleukemic SKT6 cells (Sharlow et al., 1997). Therefore, we have tested the effect of SHP-1 antisense phosphorothiorate oligonucleotide on SHP-1 expression in PC12 cells. Cells were treated with the sense or antisense oligonucleotides (10  $\mu$ M) in LipofectAMINE for various times, SHP-1 was immunoprecipitated, and the immunoprecipitates were immunoblotted with anti-SHP-1 antibody.

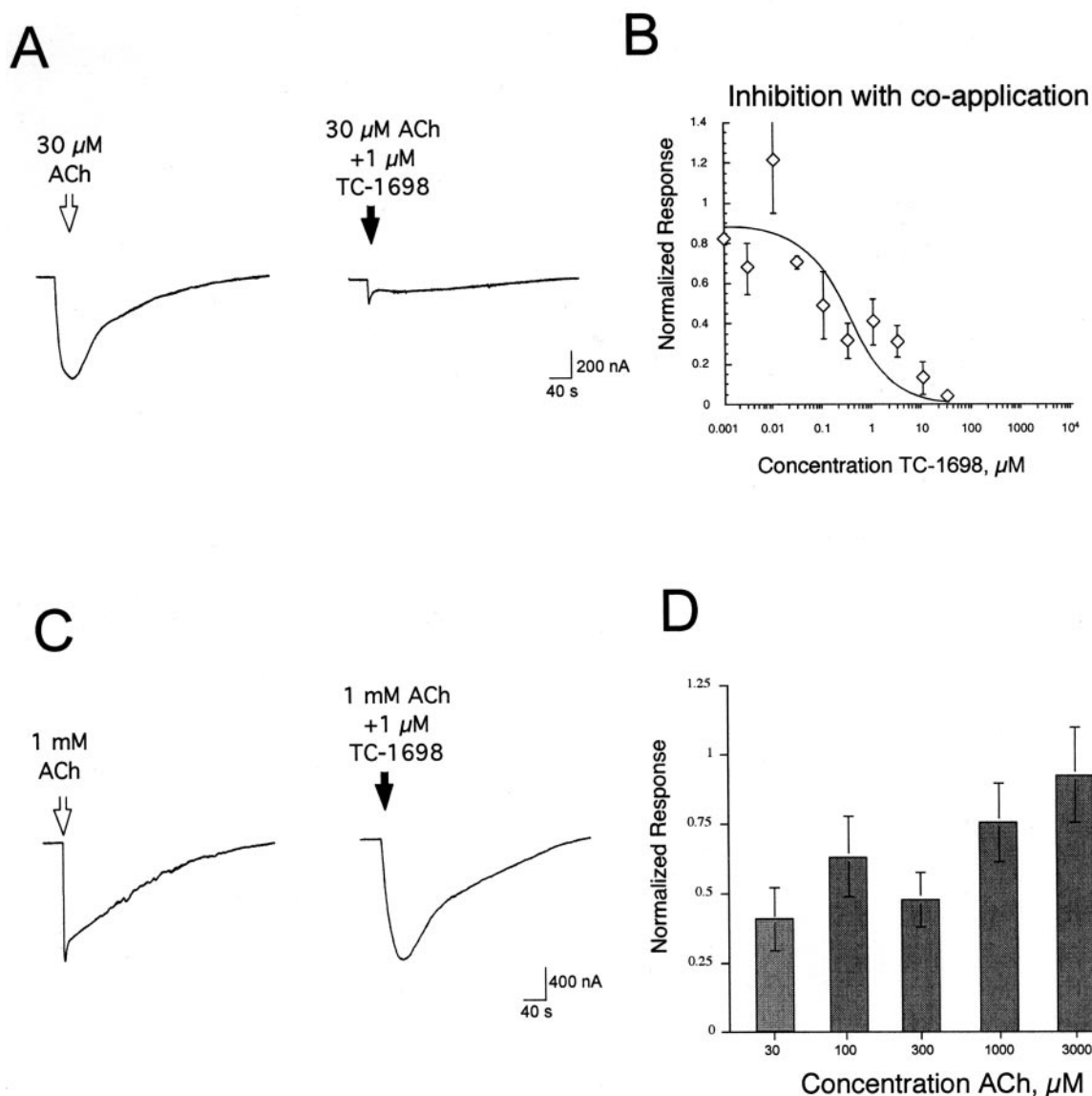
### Assessment of PC12 Cell Apoptosis

Apoptosis was determined by assessing the cleavage of the DNA-repairing enzyme PARP using a Western blot assay. PARP (116 kDa) is an endogenous substrate for caspase-3, which is cleaved to a typical 85-kDa fragment during various forms of apoptosis. PC12 cells were treated with 0.1  $\mu$ M A $\beta$  for 8 h in the presence or absence of TC-1698 and/or AG-490. The cells were collected, washed with PBS, and lysed in 1 ml of SDS-PAGE sample buffer boiled for 10 min. Total cell lysates (30  $\mu$ g of protein) were separated by SDS-PAGE and transferred to nitrocellulose membranes. The membranes were blocked for 1 h at 25°C with 5% nonfat dry milk in TBST (25 mM Tris-HCl, pH 7.5, 0.5 M NaCl, and 0.05% Tween 20). Membranes were incubated with primary PARP antibody specific for the 85-kDa fragments for 2 to 3 h at 25°C, rinsed with TBST, and incubated with secondary antibody for 1 h at 25°C. Immunodetection was performed with appropriate antibody using an enhanced chemiluminescence system (Amersham Biosciences Inc.).

Caspase 3 enzyme activity was determined with a fluorogenic substrate for caspase-3 in crude PC12 cell extracts. The caspase 3 fluorogenic peptide Ac-DEVD-AMC (Promega, Madison, WI) contains the specific caspase 3 cleavage sequence (DEVD) coupled at the C-terminal to the fluorochrome 7-amino-4-methyl coumarin. The substrate emits a blue fluorescence when excited at a wavelength of 360 nm. When cleaved from the peptide by the caspase 3 enzyme activity in the cell lysate, free 7-amino-4-methyl coumarin is released and can be detected by its yellow/green emission at 460 nm. Appropriate controls included a reversible aldehyde inhibitor of caspase 3 to assess the specific contribution of the caspase 3 enzyme activity (data not shown). Fluorescence units were normalized relative to total protein concentration of the cell extract. We performed the assays in triplicate and repeated the experiments six times.



**Fig. 2.** Effects of TC-1698 on nAChR. Responses of oocytes expressing human  $\alpha 4\beta 2$  receptors (A), human  $\alpha 7$  receptors oocytes (B), human  $\alpha 3\beta 2$  (C), mouse muscle-type receptors  $\alpha 1\beta 1\epsilon\delta$  (D), or human  $\alpha 3\beta 4$  (E). Representative raw data traces are shown on the left, and concentration-response curves to the application of either ACh or TC-1698 are shown on the right. In the concentration-response curves, each point is the mean response of at least three cells ( $\pm$ S.E.M.). Each measurement was initially normalized to the ACh control response measured in the same cell. These values were subsequently scaled by the ratio of the ACh controls to the ACh maximum response.

$\alpha 4\beta 2$  nAChR

**Fig. 3.** ACh and TC-1698 coapplication responses of  $\alpha 4\beta 2$  nAChR. A, effect of coapplication of 1  $\mu\text{M}$  TC-1698 on the response inhibition of an oocyte expressing human  $\alpha 4\beta 2$  receptors. On the left is shown the response to 30  $\mu\text{M}$  ACh alone. On the right is the response of the same oocyte to 30  $\mu\text{M}$  ACh plus 1  $\mu\text{M}$  TC-1698. B, inhibition curve for the effect of increasing concentrations of TC-1698 on the responses of  $\alpha 4\beta 2$ -expressing oocytes to the application of 30  $\mu\text{M}$  ACh coapplied with TC-1698. Each point is the mean response of at least three cells ( $\pm$ S.E.M.). Each measurement is expressed relative to the ACh control response measured in the same cell before the coapplication of ACh and TC-1698. C, peak responses to high concentrations of ACh are relatively unaffected by coapplication of TC-1698. On the left is shown the response to 1 mM ACh alone. On the right is the response of the same oocyte to 1 mM ACh plus 1  $\mu\text{M}$  TC-1698. D, effect of 1  $\mu\text{M}$  TC-1698 on the inhibition of responses to varying concentrations of ACh coapplied to oocytes expressing human  $\alpha 4\beta 2$  receptors. Data are normalized to the responses of the same oocytes to ACh alone applied at the indicated concentrations. Each bar is the mean response of at least three cells ( $\pm$ S.E.M.).

### Data Analysis

All statistical comparisons were made using Student's *t* test for paired data and analysis of variance. Significance was  $p < 0.05$ .

## Results

### Electrophysiological Studies Indicate That TC-1698 Is a Selective Agonist to the $\alpha 7$ nAChR

**$\alpha 4\beta 2$  nAChR.** TC-1698 had little or no agonist activity when applied alone at concentrations up to 100  $\mu\text{M}$  to oocytes

expressing  $\alpha 4\beta 2$  receptors (<3% ACh maximum; Fig. 2). However, subsequent to the application of TC-1698, we noted that subsequent ACh control responses were progressively inhibited ( $\text{IC}_{50} > 30 \mu\text{M}$ , Fig. 3). Because we noted an inhibition of  $\alpha 4\beta 2$  control ACh responses after the application of TC-1698, we further investigated whether TC-1698 might function as an antagonist of  $\alpha 4\beta 2$  nAChR. When TC-1698 was coapplied at increasing concentration with 30  $\mu\text{M}$  ACh, we noted a concentration-dependent inhibition of the ACh response ( $\text{IC}_{50} \approx 300 \text{ nM}$ ; Fig. 3). To further investigate the

TABLE 1

Binding selectivity profile of TC-1698

Data are mean percent inhibition of control binding (or activity) for duplicate determinations. No data denotes less than 25% change in binding at 10  $\mu$ M TC-1698. For all non-nicotinic receptors tested, TC-1698 had an  $IC_{50} > 1 \mu$ M.

Binding Site	Radioligand	Inhibition (Percentage at 10 $\mu$ M)
Acetylcholinesterase	Acetylthiocholine	
Adenosine, nonselective	[ <sup>3</sup> H]NECA	
Adrenergic $\alpha_1$ (rat cortex)	[ <sup>3</sup> H]MeOxy-prazocin	
Adrenergic $\alpha_2$ (rat cortex)	[ <sup>3</sup> H]RX-821002	
Adrenergic $\beta$ nonselective	[ <sup>3</sup> H]DHA	
Angiotensin AT <sub>1</sub> (human)	[ <sup>125</sup> I]-(Sar1-Ile8) angiotensin	
Angiotensin AT <sub>2</sub>	[ <sup>125</sup> I]Tyr4-angiotensin II	
Calcium channel, type L	[ <sup>3</sup> H]Nitrendipine	
Bradykinin, BK2	[ <sup>3</sup> H]Bradykinin	
Calcium channel, type N	[ <sup>3</sup> H]conotoxin GVIA	
Cholecystokinin, CCK1 (CCKA)	[ <sup>125</sup> I]CCK-8	
Cholecystokinin, CCK2 (CCKB)	[ <sup>125</sup> I]CCK-8	
Choline acetyltransferase	[ <sup>14</sup> C]-Acetyl Coenzyme	
Glutamic acid decarboxylase	[ <sup>14</sup> C]-Glutamic Acid	
Corticotropin-releasing factor	[ <sup>3</sup> H]-Tyr0-oCRF	
Dopamine D3 (rat recombinant)	[ <sup>3</sup> H]Spiperone	
Dopamine transporter	[ <sup>3</sup> H]-WIN 35,428	
Endothelin ET-A (Human)	[ <sup>125</sup> I]-Endothelin1	
Endothelin ET-B (Human)	[ <sup>125</sup> I]-Endothelin1	
GABA (rat cortex)	[ <sup>3</sup> H]-GABA	
Estrogen	[ <sup>125</sup> I] 3,17B-Estradiol, 16a	
GABA-A, BDZ, $\alpha$ 1, central	[ <sup>3</sup> H]-Flunitrazepam	
GABA-B transporter (rat cortex)	[ <sup>3</sup> H]-CGP 5462A	
Galanin, nonselective	[ <sup>125</sup> I] Galanin	
Glycine (rat spinal cord)	[ <sup>3</sup> H]-Strychnine	
Histamine H1 periph. (guinea pig lung)	[ <sup>3</sup> H]-Pyrilamine	
Histamine H1	[ <sup>3</sup> H]-Pyrilamine	
Histamine H2	[ <sup>3</sup> H]-Pyrilamine	39
Histamine H3	[ <sup>3</sup> H]-Pyrilamine	60
Leukotriene B4, LTB4	[ <sup>3</sup> H]-LTB4	
Leukotriene D4, LTD4	[ <sup>3</sup> H]-LTD4	
Melatonin ML1 (chicken brain)	[ <sup>125</sup> I]-Iodomelatonin	
Monoamine oxidase A, peripheral	[ <sup>14</sup> C]-5HT	
Monoamine oxidase B, peripheral	[ <sup>14</sup> C]phenylethylamine	
Muscarinic, M1 (human recombinant)	[ <sup>3</sup> H]-QNB	
Muscarinic, M2 (human recombinant)	[ <sup>3</sup> H]-QNB	46
Muscarinic, nonselective central	[ <sup>3</sup> H]-QNB	
Muscarinic, nonselective, peripheral	[ <sup>3</sup> H]-QNB	
Neurokinin, NK1	[ <sup>3</sup> H]-SP	
Neurokinin, NK2 (human recombinant)	[ <sup>3</sup> H]-NKA	
Neurokinin, NK3 (NKB)	[ <sup>3</sup> H]-Eledoisin	
Nicotinic (rat cortex)	[ <sup>3</sup> H]-Cytisine	104
Norepinephrine transporter (rat cortex)	[ <sup>3</sup> H]-Nisoxetine	
NOS (neuronal-binding)	[ <sup>3</sup> H]-NOARG	
Opioids (rat cortex)	[ <sup>3</sup> H]-Naloxone	
Oxytocin (rat uterus)	[ <sup>3</sup> H]-oxytocin	
Platelet-activating factor, PAF	Hexadecyl-[ <sup>3</sup> H]-acetyl-PAF	
Potassium K <sub>ATP</sub> channels (rat cortex)	[ <sup>3</sup> H]-Glibenclamide	
Potassium K <sub>VI</sub> channels (rat cortex)	[ <sup>125</sup> I]-Apamin	
Potassium K <sub>VS</sub> channels (rat cortex)	[ <sup>125</sup> I]-Charybdotoxin	
Serotonin transporter	[ <sup>3</sup> H]-Citalopram, N-methyl	
Serotonin, nonselective	[ <sup>125</sup> I]-LSD	
Sigma (rat cortex)	[ <sup>3</sup> H]-DTG	35
Sodium channels site 2 (rat cortex)	[ <sup>3</sup> H]-Batrachotoxin	
Testosterone (cytosolic)	[ <sup>3</sup> H]-Methyltrienolone	
Thromboxane A2 (Human)	[ <sup>3</sup> H]-SQ 29,548	
Thyrotropin-releasing hormone, TRH	[ <sup>3</sup> H]-(3MeHis2)TRH	
Vasoactive intestinal peptide	[ <sup>125</sup> I]-VIP	
Vasopressin V <sub>1</sub> (rat aortic A7r5 cells)	[ <sup>3</sup> H]-AVP	

nature of the TC-1698 inhibition of  $\alpha 4\beta 2$  ACh responses, we conducted some competition experiments. We noted that when TC-1698 at a fixed concentration of 1  $\mu$ M was coapplied with increasing concentrations of ACh, there was inhibition of the response to low concentrations of ACh but not to high concentrations of ACh, consistent with competitive inhibition (Fig. 3; Table 1).

**$\alpha 3\beta 2$  nAChR.** TC-1698 also had relatively little activity when applied alone at concentrations up to 300  $\mu$ M to oocytes

expressing  $\alpha 3\beta 2$  receptors (<5% ACh maximum; Fig. 2; Table 1). However, subsequent ACh responses were decreased after TC-1698 was applied alone ( $IC_{50} \approx 25 \mu$ M; data not shown).

**$\alpha 3\beta 4$  nAChR.** When TC-1698 was applied to oocytes expressing  $\alpha 3\beta 4$  receptors, very small currents were observed at very high concentrations ( $I_{max} \approx 5\%$  that of ACh,  $EC_{50} = 1600 \mu$ M; Fig. 2). After the application of TC-1698 to oocytes expressing  $\alpha 3\beta 4$  receptors, little or no inhibition of subsequent ACh control responses was observed (data not shown).

**$\alpha 1\beta 1\epsilon\delta$  nAChR.** TC-1698 was also a relatively potent and modestly efficacious agonist of mouse muscle nAChR expressed in *Xenopus* oocytes. The maximum current was  $28 \pm 1\%$  of the maximum response to ACh. TC-1698 had an  $EC_{50}$  value of  $20 \pm 1.3 \mu\text{M}$ , 50 times less potent than for  $\alpha 7$ , compared with  $82 \mu\text{M}$  for ACh (Fig. 2).

**$\alpha 7$  nAChR.** Whereas TC-1698 had very little agonist activity with  $\beta$ -subunit-containing neuronal nAChR, it seemed to be a potent and efficacious agonist of  $\alpha 7$ -type receptors. It produced maximum responses equivalent to those produced by ACh (i.e.,  $I_{\text{max}} \geq 100\%$  compared to ACh). TC-1698 was approximately 30-fold more potent than ACh, with an  $EC_{50}$  value of  $440 \pm 14 \text{ nM}$ , compared with  $30 \mu\text{M}$  for ACh (Fig. 2). TC-1698 application to  $\alpha 7$ -expressing oocytes produced no significant residual inhibition of subsequent ACh responses (data not shown). In Fig. 2A, note that because TC-1698 is a far more potent agonist than ACh, although the TC-1698 peak current is larger than that of the ACh controls, the net charge is roughly equivalent to that evoked by the  $300 \mu\text{M}$  ACh control.

### Activity Profile for TC1698 in Clonal Cells

The affinity of TC-1698 for brain nAChR was determined by radioligand binding studies. Membranes prepared from rat hippocampus, a brain region enriched in  $\alpha 7$  nAChR, were used along with [ $^3\text{H}$ ]MLA as labeling agent and TC-1698 exhibited a  $K_i$  of  $11 \pm 1.7 \text{ nM}$  in this preparation ( $n = 4$ ). The potency and efficacy of TC-1698 at peripheral nAChR was assessed using radioactive rubidium efflux assays in rat and human cell lines expressing muscle- and ganglion-type nAChR (Lukas and Cullen, 1988). TC-1698 is a poor activator of rat and human ganglion-type nAChR and human muscle type receptors expressed in clonal cell lines. At  $100 \mu\text{M}$ , activation of either human muscle receptor (human TE671/RD) or ganglion-type receptors (rat PC12 and human SH-SY5Y cells) were below 20% of that of nicotine. The intrinsic activity of TC-1698 at brain nAChR was assessed using [ $^3\text{H}$ ]dopamine release from rat striatal synaptosomes. TC-1698 resulted in no significant activation of dopamine release, suggesting a lack of agonist activity at  $\alpha 4\beta 2$  nAChR.

A binding profile was conducted to evaluate the interaction of TC-1698 with other receptors, transporters, enzymes, or ion channels. With the exception of nicotinic receptors at which binding was totally displaced,  $10 \mu\text{M}$  TC-1698 had no or very low affinity for all binding sites examined (Table 2).

TABLE 2  
Activation parameters for TC-1698

	$I_{\text{max}}$	$n$	$EC_{50}$
$\alpha 4\beta 2$	<0.05	NA <sup>a</sup>	(.03 ACh $I_{\text{max}}$ @ $100 \mu\text{M}$ )
$\alpha 7$	1.0	0.9	$345 \pm 110 \text{ nM}$
$\alpha 3\beta 2$	$\leq 0.06$	NA <sup>a</sup>	(0.05–0.02 ACh $I_{\text{max}}$ 30–300 $\mu\text{M}$ ) <sup>a</sup>
$\alpha 1\beta 1\epsilon\delta$	0.28	2.0	$20 \pm 1.3 \mu\text{M}$
$\alpha 3\beta 4$	<0.05	NA <sup>a</sup>	(.02 ACh $I_{\text{max}}$ @ $1 \text{ mM}$ )

<sup>a</sup> NA, not available, that is, the responses were too low for the data to give a meaningful curve fit.

<sup>b</sup> Between 30 and  $300 \mu\text{M}$  there were detectable responses that varied between 0.05 and 0.02 of the ACh maximum response; however, responses to  $30 \mu\text{M}$  and  $100 \mu\text{M}$  were not statistically different and responses to  $300 \mu\text{M}$  were, if anything, less than the responses to 100 and  $30 \mu\text{M}$ .

### Effects of the JAK2 Inhibitor AG-490 on TC-1698-Induced Tyrosine Phosphorylation of JAK2 and PI-3-Kinase and Serine Phosphorylation of Akt in PC12 Cells

Enzymatic activation of JAK2 was determined via its tyrosine phosphorylation. The tyrosine phosphorylated JAK2 sometimes shows up as a doublet or shifts in its migration in the SDS-PAGE gel. These anomalies may be due to either proteolysis of JAK2 or different levels of serine phosphorylation of the enzyme (Marrero et al., 1998; Shaw et al., 2002). In this study, we found that JAK2 is tyrosine phosphorylated in response to the  $\alpha 7$  receptor specific ligand TC-1698 ( $10 \mu\text{M}$ ) within 5 min, and this activation remained above basal levels even after longer exposure (60 min) to compound TC-1698 (Fig. 4). We also found that preincubation for 1 h with the JAK2 inhibitor AG-490 ( $10 \mu\text{M}$ ) inhibited the TC-1698-induced JAK2 tyrosine phosphorylation, the tyrosine phosphorylation of PI-3-K, and the serine phosphorylation of Akt (Fig. 4). These results are similar in their kinetics of JAK2 activation to our previous reported results when we used nicotine (Shaw et al., 2002).

### Effects of Ang II Pretreatment with or without Ang II Receptor Antagonists on TC-1698-Induced Tyrosine Phosphorylation of JAK2

Preincubation of PC12 cells with Ang II blocked TC-1698-induced tyrosine phosphorylation of JAK2 (Fig. 5A). This inhibition was completely prevented by preincubation with an  $AT_2$  antagonist (PD 123177 at  $100 \text{ nM}$ ) but not by an  $AT_1$  antagonist (candesartan at  $100 \text{ nM}$ ) (Fig. 5A), consistent with the Ang II receptor phenotype expressed in PC12 cells. Consistent with our data indicating that TC-1698 is a potent selective agonist of  $\alpha 7$ -type receptors, TC-1698-induced activation of JAK2 was blocked by the  $\alpha 7$  antagonist  $\alpha$ -bungarotoxin (Fig. 5C).

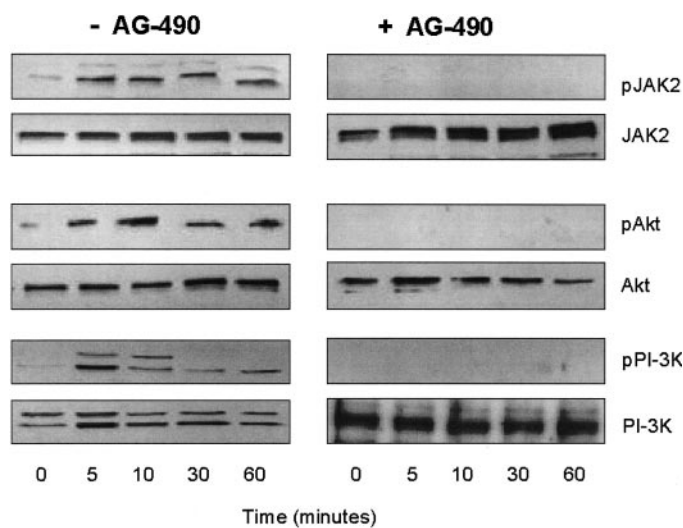


**Fig. 4.** TC-1698-induced activation of JAK2, Akt, and PI-3-kinase in PC12 cells in the presence or absence of AG-490. PC12 cells preincubated in the presence or absence of the JAK2 inhibitor AG-490 ( $10 \mu\text{M}$ ) were stimulated with  $10 \mu\text{M}$  TC-1698 for the time indicated. Cells were immunoblotted with phospho-specific and nonphosphospecific anti-JAK2 and anti-Akt antibodies or with anti-PI-3-kinase antibody. The PI-3-kinase immunoprecipitated proteins were then immunoblotted with anti-phosphotyrosine and anti-PI-3-kinase antibodies. Results shown for each immunoblot is representative of three immunoblots.

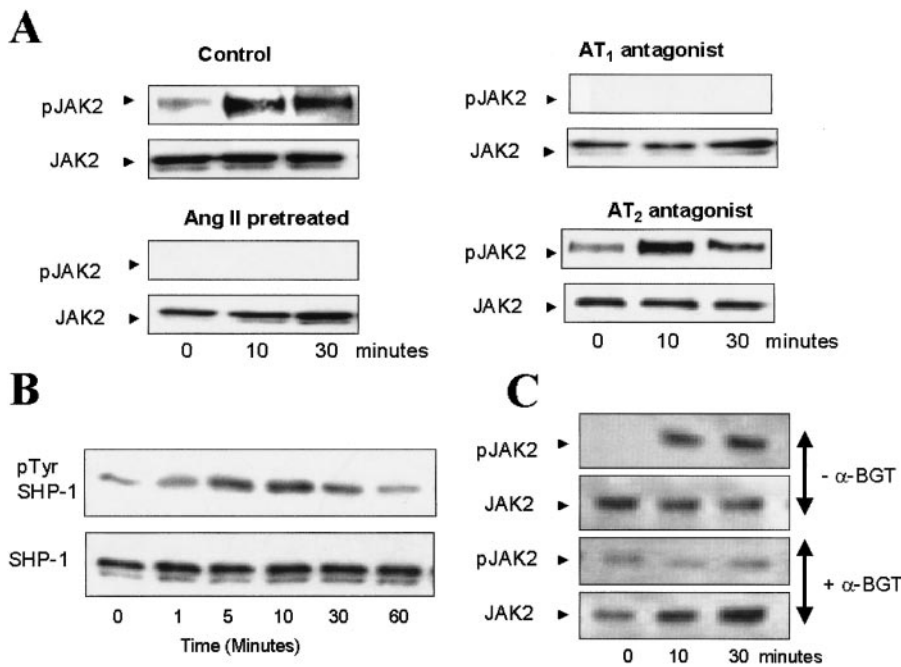


**Fig. 5.** A, effects of Ang II pretreatment with or without Ang II receptor antagonists on the TC-1698-induced activation of JAK2 in PC12 cells. Cells preincubated with Ang II for 8 h in the presence or absence of AT<sub>1</sub> antagonist candesartan or AT<sub>2</sub> antagonist PD 123177 were stimulated with TC-1698 for the time indicated. Cells were immunoblotted with phospho-specific and nonphosphospecific anti-JAK2. Results shown for each immunoblot is representative of three immunoblots. B, angiotensin II-induced phosphorylation of SHP-1 in PC12 cells. PC12 cells were incubated for 24 h in serum-free medium before exposure to Ang II (100 nM) for the times indicated. Cells were lysed, and SHP-1 was immunoprecipitated from lysates with 10  $\mu$ g/ml anti-SHP-1 monoclonal antibodies and immunoblotted with anti-phosphotyrosine antibody. Results shown for each immunoblot are representative of three immunoblots. C, effects of  $\alpha$ -bungarotoxin on TC-1698-stimulated JAK2 phosphorylation. Cells preincubated with 0.1  $\mu$ M  $\alpha$ -bungarotoxin or vehicle followed by addition of 0.1  $\mu$ M TC-1698 for the times indicated. Results shown for each immunoblot is representative of three immunoblots.

### Ang II-Induced Activation and Tyrosine Phosphorylation of SHP-1 and Its Effects on TC-1698-Induced Tyrosine Phosphorylation of JAK2

The AT<sub>2</sub> receptor exerts growth-inhibitory effects in cultured cells and in vivo, one of which has been proposed to be programmed cell death (Horiuchi et al., 1998; Lehtonen et al., 1999). Despite growing interest in AT<sub>2</sub> receptor-mediated apoptosis, relatively little is known about the molecular basis of this process. Recently growth-inhibitory effects of the AT<sub>2</sub> receptor have been reported to be mediated by the activation of PTPases, AT<sub>2</sub> receptor stimulation is associated with a rapid activation of SHP-1 in rat pheochromocytoma PC12 cells (Horiuchi et al., 1998). However, at present, no functional role has been demonstrated for SHP-1 activation by the AT<sub>2</sub> receptor, and it is interesting to note that SHP-1 has been shown to function as a negative regulator of JAK2 signaling (Marrero et al., 1998). Therefore, the potential biological significance of AT<sub>2</sub> receptor-induced programmed cell death led us to investigate whether SHP-1 activation could be involved in this process. We found that Ang II induced both the tyrosine phosphorylation and activation of SHP-1 (Fig. 5B) and that vanadate, a specific inhibitor of PTPases (Marrero et al., 1996), blocked the activation of SHP-1 directly (Fig. 6). Furthermore, vanadate also augmented TC-1698-induced tyrosine phosphorylation of JAK2 (Fig. 6).

### Antisense against SHP-1 and Its Effects on TC-1698-Induced Tyrosine Phosphorylation of JAK2 in PC12 Cells

Because vanadate is not a specific inhibitor of SHP-1, we also tested the effect of SHP-1 antisense phosphorothioate oligonucleotide on SHP-1 expression in PC12 cells. Cells were treated with the sense, or antisense oligonucleotides (10  $\mu$ M) for various times, SHP-1 was immunoprecipitated, and the immunoprecipitates were immunoblotted with anti-SHP-1 antibody. As shown in Fig. 7A, the antisense (but not the sense) oligonucleotide was effective in completely inhibiting SHP-1 expression within 12 h. We then tested whether these

antisense oligos could be used to regulate the TC-1698-induced activation JAK2 in PC12 cells. PC12 cells were stimulated with Ang II and lysed. JAK2 was then immunoprecipitated from lysates with anti-JAK2 antibody. Immunoprecipitated proteins were separated by gel electrophoresis, transferred to nitrocellulose, and then immunoblotted with anti-phosphotyrosine antibody. As a control, cells were exposed to SHP-1 sense oligonucleotide. As shown in Fig. 7B, when cells were exposed to the SHP-1 antisense form 12 h, JAK2 tyrosine phosphorylation was augmented. These results suggest that SHP-1 is the PTPase that dephosphorylates JAK2 after TC-1698-induced JAK2 phosphorylation in PC12 cells.

### Assessment of PC12 Cell Apoptosis

Apoptosis was determined by assessing the cleavage of the DNA-repairing enzyme PARP using a Western blot assay. PC12 cells were treated with 0.1  $\mu$ M A $\beta$  for 8 h in the presence or absence of TC-1698 (10  $\mu$ M). As shown in Fig. 8, PARP (116 kDa) was cleaved to its 85-kDa fragment after A $\beta$  (1-42) treatment. The A $\beta$  (1-42)-induced cleavage of PARP was blocked by TC-1698, which was prevented by preincubation with AG-490 or Ang II (Fig. 8). Further 12-h pretreatment with SHP-1 antisense, but not sense, completely prevented the cleavage of PARP (compare lanes 8 and 10). These results support our main hypothesis, which states that JAK2 plays a central role in the nicotinic  $\alpha$ 7 receptor-induced neuroprotection, which Ang II blocks through the AT<sub>2</sub> receptor activation of the PTPase SHP-1.

Apoptosis was also determined by activation of caspase 3. Caspase 3 is expressed in PC12 cells and is known to be involved in apoptosis (Shaw et al., 2002). Therefore, we examined caspase 3 activity after Ang II-induced apoptosis. We used the fluorescent peptide substrate Ac-DEVD-7AMC to measure caspase 3-like activity in cell lysates. As shown in Fig. 9, the caspase 3-like activity that resulted in the cleavage of the peptide substrate Ac-DEVD-7AMC is evident after 2 h of Ang II treatment and increased over time until it

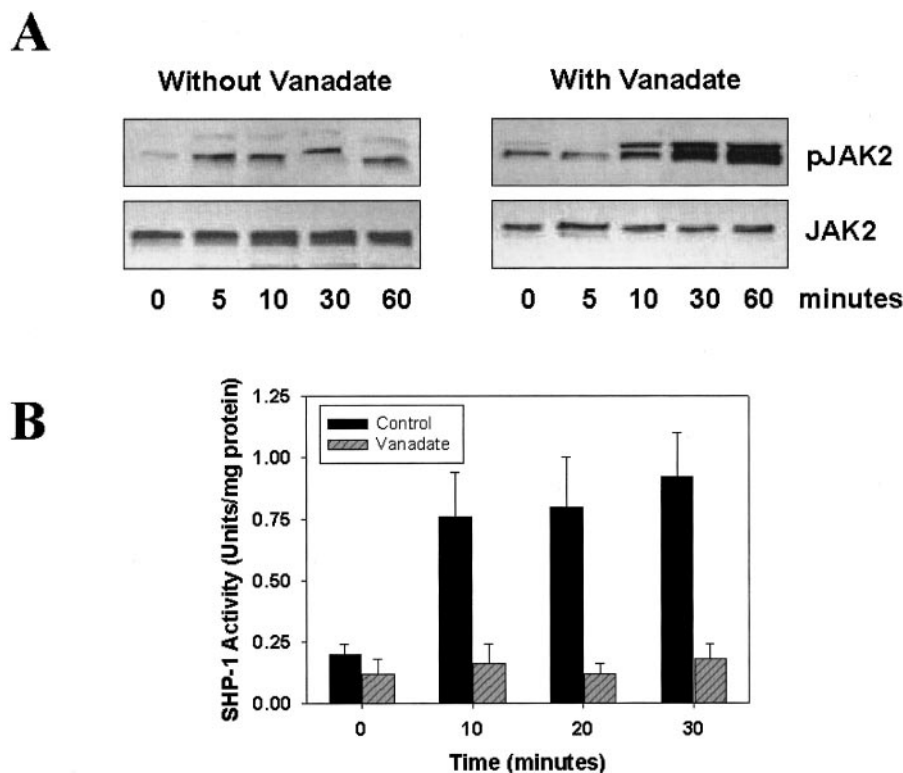


**Fig. 6.** A, TC-1698-induced activation of JAK2 in PC12 cells in the absence or presence of vanadate. PC12 cells preincubated in the presence or absence of the tyrosine phosphatase vanadate were stimulated with TC-1698 for the times indicated. Cells were immunoblotted with phospho-specific and nonphospho-specific anti-JAK2. B, time-dependent increase in SHP-1 activity in the absence or presence of vanadate. Results shown for each immunoblot is representative of three immunoblots.

reached a peak after 8 h of treatment. However, the Ang II-induced activation of caspase 3 was blocked significantly in the presence of SHP-1 antisense (+,  $P < 0.01$ ) or vanadate (\*,  $P < 0.01$ ) (Fig. 9). Coincubation with the SHP-1 sense had no effect on the Ang II-induced activation of caspase 3. In addition, incubation with TC-1698 had also no effect caspase 3 activation (Fig. 9).

### Discussion

In this study, we found that TC-1698, a novel  $\alpha 7$ -selective ligand, exerted neuroprotective effects via activation of the JAK2/PI-3K cascade, which can be neutralized through activation of the Ang II  $AT_2$  receptor. The Ang II  $AT_2$  receptor effects are reversed by nullifying a PTPase as evidenced by the usage of the PTPase-specific inhibitor vanadate (Marrero et al., 1996). Vanadate not only augmented the TC-1698-induced tyrosine phosphorylation of JAK2 but also blocked the Ang II neutralization of TC-1698-induced neuroprotection against  $A\beta$  (1-42)-induced cleavage of PARP. Furthermore, when we also neutralized SHP-1 via antisense transfection the Ang II neutralization of TC-1698-induced neuroprotection against  $A\beta$  (1-42) was again blocked. These results support our main hypothesis, which states that JAK2 plays a central role in the nicotinic  $\alpha 7$  receptor-induced activation of the JAK2-PI-3K cascade in PC12 cells, which ultimately contribute to nAChR-mediated neuroprotection. Furthermore, we also found that Ang II blocked this pathway through the  $AT_2$  receptor activation of SHP-1 (Fig. 10).

TC-1698 was relatively potent as an antagonist of the ACh responses of  $\alpha 4\beta 2$  receptors, apparently working through a competitive mechanism. TC-1698 also blocked subsequent ACh control responses of  $\alpha 4\beta 2$  and  $\alpha 3\beta 2$  receptors after it was applied in the absence of ACh. Interestingly, TC-1698 seems to be a full potent agonist only for the  $\alpha 7$  receptors.

TC-1698 should predominantly activate  $\alpha 7$  and inhibit  $\alpha 4\beta 2$  with relatively little effect on other receptors. TC-1698 seems to be a weak partial agonist/antagonist of beta subunit-containing neuronal receptors. The studies were conducted in PC12 cells with similar effects to those observed in human SH-SY5Y cells. Both of these cell lines exhibit  $\alpha 7$ - and  $\alpha 3\beta 4$ -containing receptors and TC-1698 interacts with the former but not the latter.

Several reports have documented the apoptotic effects of Ang II through  $AT_2$  receptors.  $AT_2$  receptors are expressed in PC12 and have been shown to inhibit the JAK/STAT signaling cascade (Kunioku et al., 2001). In contrast to nicotine-induced neuroprotection against  $\beta$ -amyloid (1-42), pretreatment of cells with Ang II blocks nicotine-induced activation of JAK2 via the  $AT_2$  receptor and completely prevents nicotine-mediated neuroprotective effects, further suggesting a pivotal role for JAK2 phosphorylation (Shaw et al., 2002). Our findings in this study are consistent with the opposite roles on cell viability that exist between the  $\alpha 7$  nAChR and the  $AT_2$  receptor with activation of the  $AT_2$  receptor overriding the potential benefit through the  $\alpha 7$  nAChR. These results and the convergence of these pathways on phosphorylated JAK2 suggest that recruitment of nicotinic  $\alpha 7$  nAChR receptor-mediated neuroprotection against  $A\beta$  (1-42) may be optimized under conditions where the  $AT_2$ -mediated inhibition is minimized by blocking the  $AT_2$ -induced activation of the PTPase SHP-1. Therefore, the findings in this study identify novel molecular mechanisms, which are fully consistent with the role attributed to  $\alpha 7$  nAChR-induced activation of JAK2 and subsequent neuroprotective effect,  $AT_2$ -induced activation of SHP-1, and its purported role in apoptotic events.

SHP-1 is a soluble tyrosine phosphatase that participates in the negative regulation of the tyrosine kinase JAK2 (Marrero et al., 1998), and it has been recently reported that

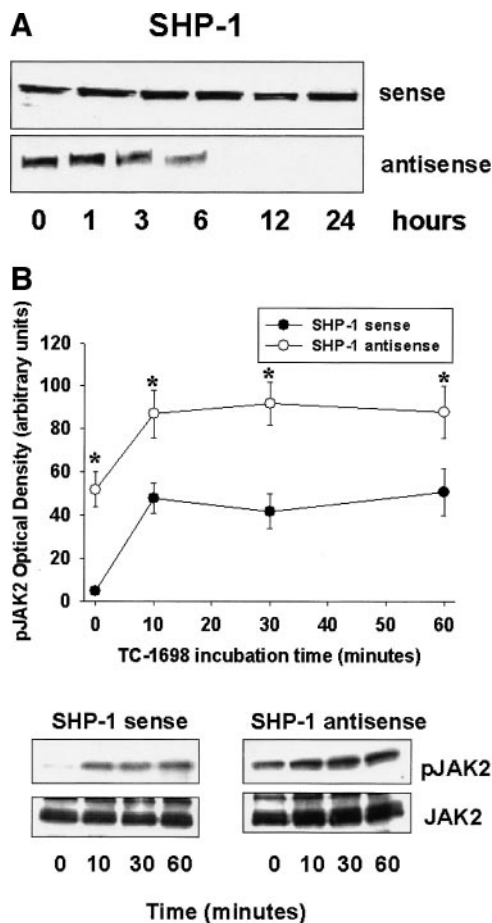


**Fig. 7.** A, effects of SHP-1 sense and antisense oligonucleotides on SHP-1 expression in PC12 cells. PC12 cells were treated with SHP-1 sense and antisense oligonucleotides for the times indicated and lysed. SHP-1 was immunoprecipitated from the lysates with anti-SHP-1 antibody. Precipitated SHP-1 proteins were then immunoblotted with specific anti-SHP-1 antibody. Results shown for each immunoblot are representative of three immunoblots. B, effects of SHP-1 antisense on the TC-1698-induced activation of JAK2 in PC12 cells. Cells preincubated in the presence or absence of SHP-1 antisense or sense oligonucleotides were stimulated with TC-1698 for the times indicated. Cells were immunoblotted with phospho-specific and nonphospho-specific anti-JAK2. Results shown for each immunoblot are representative of three immunoblots.

stimulation of AT<sub>2</sub> receptors rapidly activates SHP-1 in N1E-115 and AT<sub>2</sub>-transfected Chinese hamster ovary cells (Horiuchi et al., 1998; Lehtonen et al., 1999). In the present study, we document that the Ang II AT<sub>2</sub> receptor activates SHP-1 in PC12 and that the TC-1698-induced activation of JAK2 is augmented by SHP-1 antisense transfection. These results suggest that both SHP-1 activation and JAK2 deactivation constitute sequential events in the same signaling pathway.

Nicotinic neurotransmission is compromised in the brains of Alzheimer's disease patients and accumulating evidence suggests that nAChR-selective ligands can offer neuroprotective effects in several in vitro models, including neuronal death resulting from  $\beta$ -amyloid toxicity, *N*-methyl-D-aspartate-mediated cytotoxicity, or growth factor deprivation, and in in vivo models, including chemically induced neurotoxicity (1-methyl-4-phenyl-1,2,3,6-tetrahydropyridine models and systemic kainic acid-induced excitotoxic effects). Nicotinic ligands reduce  $\beta$ -amyloid aggregation and toxicity and inhibit amyloid deposition in transgenic mice with APPsw (Nordberg et al., 2002). A recent report has demonstrated

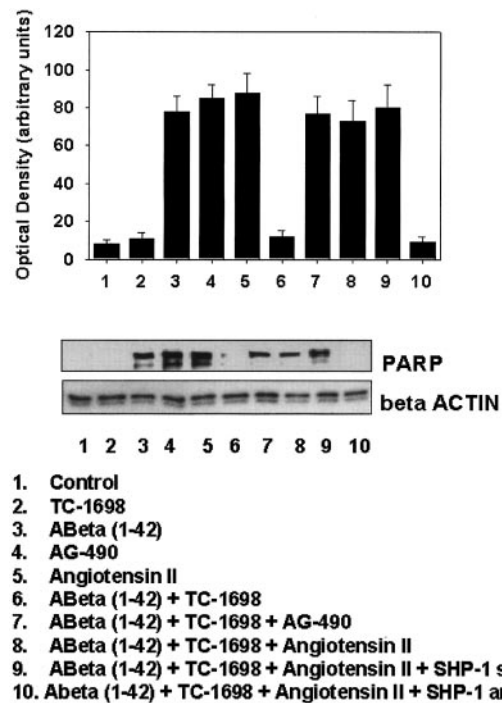


**Fig. 8.** Effects of SHP-1 antisense on TC-1698-induced protection against A $\beta$ - and Ang II-induced apoptosis. PARP expression was measured from lysates of cells treated with A $\beta$  (1-42) peptide and/or Ang II in the presence or absence of TC-1698 and/or SHP-1 antisense. Results shown for each immunoblot are representative of three immunoblots.

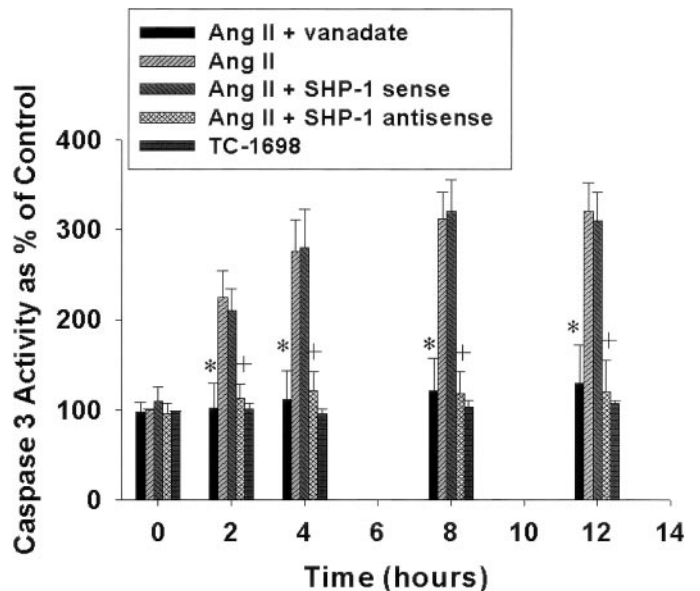


**Fig. 9.** Effects of SHP-1 antisense on the angiotensin II-induced activation of caspase-3. PC12 cells were incubated for the duration shown with Ang II in the presence of either SHP-1 antisense or SHP-1 sense or vanadate. Caspase-3 activities are shown as the mean  $\pm$  S.E. of six independent cultures.

that the  $\alpha 7$  nAChR is also an essential regulator of inflammation and is required for inhibition of cytokine release (Wang et al., 2003). The physiological mechanism coined "the cholinergic anti-inflammatory pathway", which has been proposed to have major implications in immunology and therapeutics, remains unknown. The induction and resolution of inflammatory processes are the complex outcome of interplay

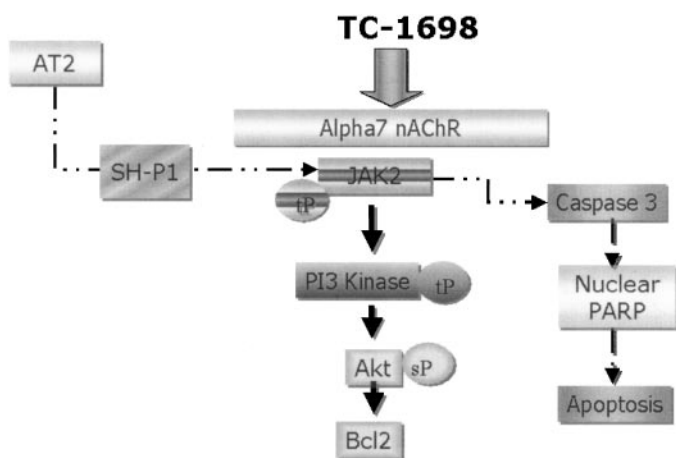


**Fig. 10.** Schematic of the protein tyrosine phosphatase SHP-1 inhibition of the  $\alpha 7$ -JAK2 survival pathway.

between pro- and anti-inflammatory cytokines. Pleiotropic cytokines such as IL-6 and IL-10 have been shown to activate the JAK-signal transducer and activator of transcription pathway and act in opposition to effects mediated by the proinflammatory cytokines IL-1 and tumor necrosis factor- $\alpha$  (Ahmed and Ivashkiv, 2000). It is conceivable from these findings that multifaceted therapeutic potential targeting cognitive deficits, neuroprotection, and inflammation in neurodegenerative diseases can be recruited through a single pharmacology targeting the  $\alpha 7$  nAChR. It remains to be established whether similar pathways are operative for these various end-points in vivo and whether the negative influence of AT<sub>2</sub> stimulation is clinically relevant. However, the putative beneficial effects of angiotensin-converting enzyme inhibitors in Alzheimer's disease and the observation of selective up-regulation of AT<sub>2</sub> receptor density (Ge and Barnes, 1996) and biosynthetic enzymes (Narain et al., 2000; Savaskan et al., 2001) concurrent with down-regulation of nAChR in the temporal cortex of some Alzheimer's disease patients (Court et al., 2001) are consistent with the opposite effects on cell viability observed in our studies through activation of AT<sub>2</sub> and  $\alpha 7$ -nAChR.

#### Acknowledgments

We thank Julia Porter Papke, Irena Garic, Bernadette Schoneburg, and Clare Stokes for technical assistance. We are very grateful to Axon Instruments for the use of an OpusXpress 6000A and pClamp 9. We particularly thank Dr. Cathy Smith-Maxwell for support and help with OpusXpress.

#### References

- Ahmed ST and Ivashkiv LB (2000) Inhibition of IL-6 and IL-10 signaling and Stat activation by inflammatory and stress pathways. *J Immunol* **165**:5227–5237.
- Bencherif M, Lovette ME, Fowler KW, Arrington S, Reeves L, Caldwell WS, and Lippello PM (1996) RJR-2403: a nicotinic agonist with CNS selectivity I. In vitro characterization. *J Pharmacol Exp Ther* **279**:1413–1421.
- Bencherif M and Schmitt JD (2002) Targeting neuronal nicotinic receptors: a path to new therapies. *CNS Neurol Disord* **1**:319–327.
- Breese CR, Adams C, Logel J, Drebing C, Rollins Y, Barnhart M, Sullivan B, Demasters BK, Freedman R, and Leonard S (1997) Comparison of the regional expression of nicotinic acetylcholine receptor  $\alpha 7$  mRNA and [125I]- $\alpha$ -bungarotoxin binding in human postmortem brain. *J Comp Neurol* **387**:385–398.
- Court J, Martin-Ruiz C, Piggott M, Spurden D, Griffiths M, and Perry E (2001) Nicotinic receptor abnormalities in Alzheimer's disease. *Biol Psychiatry* **49**:175–184.

- Davies AR, Hardick DJ, Blagbrough IS, Potter BV, Wolstenholme AJ, and Wonnacott S (1999) Characterization of the binding of [<sup>3</sup>H]methyllycaconitine: a new radioligand for labelling  $\alpha 7$ -type neuronal nicotinic acetylcholine receptors. *Neuropharmacology* **38**:679–690.
- Dicou E, Attoub S, and Gressens P (2001) Neuroprotective effects of leptin in vivo and in vitro. *Neuroreport* **12**:3947–3951.
- Dineley KT, Westerman M, Bui D, Bell K, Ashe KH, and Sweatt JD (2001) Beta-amyloid activates the mitogen-activated protein kinase cascade via hippocampal  $\alpha 7$  nicotinic acetylcholine receptors: in vitro and in vivo mechanisms related to Alzheimer's disease. *J Neurosci* **21**:4125–4133.
- Donnelly-Roberts DL, Xue IC, Arneric SP, and Sullivan JP (1996) In vitro neuroprotective properties of the novel cholinergic channel activator (ChCA), ABT-418. *Brain Res* **719**:36–44.
- Ge J and Barnes NM (1996) Alterations in angiotensin AT1 and AT2 receptor subtype levels in brain regions from patients with neurodegenerative disorders. *Eur J Pharmacol* **297**:299–306.
- Horiuchi M, Akishita M, and Dzau VJ (1998) Molecular and cellular mechanism of angiotensin II-mediated apoptosis. *Endocr Res* **24**:307–314.
- Kem WR (2000) The brain  $\alpha 7$  nicotinic receptor may be an important therapeutic target for the treatment of Alzheimer's disease: studies with DMXBBA (GTS-21). *Behav Brain Res* **113**:169–181.
- Kihara T, Shimohama S, Sawada H, Honda K, Nakamoto T, Shibasaki H, Kume T, and Akaike A (2001)  $\alpha 7$  Nicotinic receptor transduces signals to phosphatidylinositol 3-kinase to block A beta-amyloid-induced neurotoxicity. *J Biol Chem* **276**:13541–13546.
- Kitagawa H, Takenouchi T, Azuma R, Wesnes KA, Kramer WG, Clody DE, and Burnett AL (2003) Safety, pharmacokinetics and effects on cognitive function of multiple doses of GTS-21 in healthy, male volunteers. *Neuropsychopharmacology* **28**:542–551.
- Kunioku H, Inoue K, and Tomida M (2001) Interleukin-6 protects rat PC12 cells from serum deprivation or chemotherapeutic agents through the phosphatidylinositol 3-kinase and STAT3 pathways. *Neurosci Lett* **309**:13–16.
- Lehtonen JY, Daviet L, Nahmias C, Horiuchi M, and Dzau VJ (1999) Analysis of functional domains of angiotensin II type 2 receptor involved in apoptosis. *Mol Endocrinol* **13**:1051–1060.
- Liu Q, Kawai H, and Berg DK (2001) beta-Amyloid peptide blocks the response of  $\alpha 7$ -containing nicotinic receptors on hippocampal neurons. *Proc Natl Acad Sci USA* **98**:4734–4739.
- Lukas RJ and Cullen MJ (1988) An isotopic rubidium ion efflux assay for the functional characterization of nicotinic acetylcholine receptors in clonal cell lines. *Anal Biochem* **175**:212–218.
- Marrero MB, Schieffer B, Bernstein KE, and Ling BN (1996) Angiotensin II-induced tyrosine phosphorylation in mesangial and vascular smooth muscle cells. *Clin Exp Pharmacol Physiol* **23**:83–88.
- Marrero MB, Venema VJ, Ju H, Eaton DC, and Venema RC (1998) Regulation of angiotensin II-induced JAK2 tyrosine phosphorylation: roles of SHP-1 and SHP-2. *Am J Physiol* **275**:C1216–C1223.
- Meydan N, Grunberger T, Dadi H, Shahar M, Arpaia E, Lapidot Z, Leeder JS, Freedman M, Cohen A, Gazit A, et al. (1996) Inhibition of acute lymphoblastic leukaemia by a Jak-2 inhibitor. *Nature (Lond)* **379**:645–648.
- Narain Y, Yip A, Murphy T, Brayne C, Easton D, Evans JG, Xuereb J, Cairns N, Esiri MM, Furlong RA, et al. (2000) The ACE gene and Alzheimer's disease susceptibility. *J Med Genet* **37**:695–697.
- Newhouse PA, Potter A, Kelton M, and Corwin J (2001) Nicotinic treatment of Alzheimer's disease. *Biol Psychiatry* **49**:268–278.
- Nordberg A, Hellstrom-Lindahl E, Lee M, Johnson M, Mousavi M, Hall R, Perry E, Bednar I, and Court J (2002) Chronic nicotine treatment reduces beta-amyloidosis in the brain of a mouse model of Alzheimer's disease (APPsw). *J Neurochem* **81**:655–658.
- Papke RL and Papke JKP (2002) Comparative pharmacology of rat and human  $\alpha 7$  nAChR conducted with net charge analysis. *Br J Pharmacol* **137**:49–61.
- Romano C and Goldstein A (1980) Stereospecific nicotine receptors on rat brain membranes. *Science (Wash DC)*, **210**:647–650.
- Savaskan E, Hock C, Olivier G, Bruttel S, Rosenberg C, Hulet C, and Muller-Spahn F (2001) Cortical alterations of angiotensin converting enzyme, angiotensin II and AT1 receptor in Alzheimer's dementia. *Neurobiol Aging* **22**:541–546.
- Sharlow ER, Pacifici R, Crouse J, Batac J, Todokoro K, and Wojchowski DM (1997) Hematopoietic cell phosphatase negatively regulates erythropoietin-induced hemoglobinization in erythroleukemic SKT6 cells. *Blood* **90**:2175–2187.
- Shaw S, Bencherif M, and Marrero MB (2002) Janus kinase 2, an early target of  $\alpha 7$  nicotinic acetylcholine receptor-mediated neuroprotection against Abeta-(1-42) amyloid. *J Biol Chem* **277**:44920–44924.
- Wang H, Yu M, Ochani M, Amella CA, Tanovic M, Susarla S, Li JH, Wang H, Yang H, Ulloa L, et al. (2003) Nicotinic acetylcholine receptor  $\alpha 7$  subunit is an essential regulator of inflammation. *Nature (Lond)* **421**:384–388.
- Wang HY, Lee DH, D'Andrea MR, Peterson PA, Shank RP, and Reitz AB (2000) beta-Amyloid(1-42) binds to  $\alpha 7$  nicotinic acetylcholine receptor with high affinity. Implications for Alzheimer's disease pathology. *J Biol Chem* **275**:5626–5632.

**Address correspondence to:** Dr. Merouane Bencherif, Targacept Inc., 200 East First St., Suite 300, Winston-Salem, NC 27101-4165. E-mail: merouane.bencherif@targacept.com